FULL PAPER

BJC

British Journal of Cancer (2013) 108, 2013–2020 | doi: 10.1038/bjc.2013.189

Keywords: ^{212}Pb-TCMC-trastuzumab; paclitaxel; mitotic spindle checkpoint

^{212}Pb-radioimmunotherapy potentiates paclitaxel-induced cell killing efficacy by perturbing the mitotic spindle checkpoint

K J Yong[1], D E Milenic[1], K E Baidoo[1] and M W Brechbiel*[,1]

[1]*Radioimmune and Inorganic Chemistry Section, Radiation Oncology Branch, National Cancer Institute, National Institutes of Health, 10 Center Drive MSC-1002, Room B3B69, Bethesda, MD 20892-1002, USA*

Background: Paclitaxel has recently been reported by this laboratory to potentiate the high-LET radiation therapeutic ^{212}Pb-TCMC-trastuzumab, which targets HER2. To elucidate mechanisms associated with this therapy, targeted α-particle radiation therapeutic ^{212}Pb-TCMC-trastuzumab together with paclitaxel was investigated for the treatment of disseminated peritoneal cancers.

Methods: Mice bearing human colon cancer LS-174T intraperitoneal xenografts were pre-treated with paclitaxel, followed by treatment with ^{212}Pb-TCMC-trastuzumab and compared with groups treated with paclitaxel alone, ^{212}Pb-TCMC-HuIgG, ^{212}Pb-TCMC-trastuzumab and ^{212}Pb-TCMC-HuIgG after paclitaxel pre-treatment.

Results: ^{212}Pb-TCMC-trastuzumab with paclitaxel given 24 h earlier induced increased mitotic catastrophe and apoptosis. The combined modality of paclitaxel and ^{212}Pb-TCMC-trastuzumab markedly reduced DNA content in the S-phase of the cell cycle with a concomitant increase observed in the G2/M-phase. This treatment regimen also diminished phosphorylation of histone H3, accompanied by an increase in multi-micronuclei, or mitotic catastrophe in nuclear profiles and positively stained γH2AX foci. The data suggests, possible effects on the mitotic spindle checkpoint by the paclitaxel and ^{212}Pb-TCMC-trastuzumab treatment. Consistent with this hypothesis, ^{212}Pb-TCMC-trastuzumab treatment in response to paclitaxel reduced expression and phosphorylation of BubR1, which is likely attributable to disruption of a functional Aurora B, leading to impairment of the mitotic spindle checkpoint. In addition, the reduction of BubR1 expression may be mediated by the association of a repressive transcription factor, E2F4, on the promoter region of *BubR1* gene.

Conclusion: These findings suggest that the sensitisation to therapy of ^{212}Pb-TCMC-trastuzumab by paclitaxel may be associated with perturbation of the mitotic spindle checkpoint, leading to increased mitotic catastrophe and cell death.

The development of new protocols for the treatment and management of patients with pancreatic or ovarian cancer remains a high priority (Jemal *et al*, 2007). In the management of oncology patients, combinations of radiotherapy and chemotherapy are common practice to derive a greater therapeutic response. Towards this end, many pre-clinical and clinical studies have been conducted to identify more effective cytotoxic agents or radio-sensitisers, and combinations thereof that might be translated into clinical practice (Agus *et al*, 2000; Chung *et al*, 2004; Dickler and Abrams, 2005; Ko and Tempero, 2005). Paclitaxel has activity against ovarian and pancreatic cancer, and is a recognised sensitiser of ovarian and pancreatic cancer cells/tumours to the cytotoxic effects of radiation (Steren *et al*, 1993; Liebmann *et al*, 1994; Rodriguez *et al*, 1995). Paclitaxel confers its cytotoxicity through activation of the spindle checkpoint, suppressing spindle microtubule dynamics by stabilising microtubules. The result is arrest of the cell cycle at the G2/M-phase and apoptosis (Lee *et al*, 2002; Supiot *et al*, 2005). The drug has been evaluated in combination with radiotherapy and radiolabelled antibodies, and has been shown to provide additional therapeutic benefits in

*Correspondence: Dr MW Brechbiel; E-mail: martinwb@mail.nih.gov

Received 17 January 2013; revised 14 March 2013; accepted 2 April 2013; published online 30 April 2013

animal models and in patients (Clarke *et al*, 2000; Burke *et al*, 2002; Crow *et al*, 2005; Kelly *et al*, 2007; Meredith *et al*, 2007).

Targeted α-particle therapy offers the potential for more specific tumour cell killing with less damage to surrounding normal tissue than β^--emitters. Several α-emitting radionuclides have been successfully used in radioimmunotherapy (RIT) and pre-targeted RIT. Targeted α-particle therapy with ^{212}Pb has demonstrated an enhanced therapeutic efficacy in combination with chemotherapeutics, such as gemcitabine and paclitaxel (Yong and Brechbiel, 2011). The longer-lived parental radionuclide of ^{212}Bi, ^{212}Pb, a promising α-particle emitting source, serves as an *in vivo* generator of ^{212}Bi. Studies using ^{212}Pb showed the feasibility of this isotope in RIT for the treatment of disseminated intraperitoneal disease; ^{212}Pb-TCMC-trastuzumab given as a single injection showed therapeutic efficacy, which increased with multiple injections at approximately monthly intervals (Milenic *et al*, 2004; Milenic *et al*, 2005). Gemcitabine and paclitaxel were the first two chemotherapeutic drugs evaluated in conjunction with ^{212}Pb-TCMC-trastuzumab (Milenic *et al*, 2007, 2008).

Although synergistic effects of α-emitting particles with chemotherapeutics on cancer cells have been studied, the mechanisms of cell death induced by the targeted delivery of high LET radiation *in vivo* are poorly understood (Supiot *et al*, 2005; Friesen *et al*, 2007). A recent study from this laboratory demonstrated that the reduction of cell proliferation by ^{212}Pb-TCMC-trastuzumab is associated with blocked DNA damage repair and G2/M phase arrest (Yong *et al*, 2012). To better understand the possible mechanism(s) of cell killing affected by the combination of ^{212}Pb-TCMC-trastuzumab with paclitaxel, several aspects were investigated. These included apoptosis, cell cycle progression and the mitotic checkpoint; specifically, key mitotic checkpoint proteins such as BubR1. The studies described herein demonstrate that ^{212}Pb-TCMC-trastuzumab potentiates paclitaxel-induced apoptosis in the LS-174T intraperitoneal (i.p.) xenograft model. The sensitisation by ^{212}Pb-TCMC-trastuzumab may be associated with perturbation of the mitotic spindle checkpoint, leading to increased mitotic catastrophe. The ultimate aim of studies such as this will be to incorporate the knowledge gained into the design of future clinical trials that combine α-emitter RIT and chemotherapeutics.

MATERIALS AND METHODS

Cell line. The human colon carcinoma cell line (LS-174T) was used for all *in vivo* studies. LS-174T was grown in supplemented DMEM as previously described (Tom *et al*, 1976). All media and supplements were obtained from Lonza (Walkersville, MD, USA). The cell line has been screened for mycoplasma and other pathogens before *in vivo* use according to NCI Laboratory Animal Sciences Program policy. No authentication of the cell line was conducted by the authors.

mAb conjugation and radiolabelling. Trastuzumab (Herceptin; Genentech, South San Francisco, CA, USA) was conjugated with TCMC by established methods using a 10-fold molar excess of ligand to mAb as previously reported (Chappell *et al*, 2000; Milenic *et al*, 2005). The final concentration of trastuzumab was quantified by the method of Lowry (Lowry *et al*, 1951). The number of TCMC molecules linked to protein was determined using a spectrophotometric-based assay (Dadachova *et al*, 1999). A 10-mCi ^{224}Ra/^{212}Pb generator was supplied by AlphaMed, Inc, Wrentham, MA, USA. The preparation of the generator and radiolabelling procedure has been previously described (Milenic *et al*, 2005).

Tumour model, treatment and tumour harvesting. Studies were performed with 19–21 g female athymic mice (NCI-Frederick) bearing i.p. LS-174T xenografts as previously reported (Milenic *et al*, 2005). Mice were injected i.p. with 1×10^8 LS-174T cells (viability $>95\%$) in 1 ml of DMEM. Two-days after the tumour cell inoculation, the mice were given i.p. injections of paclitaxel (600 μg; Hospira, Inc, Lake Forest, IL, USA). ^{212}Pb-TCMC-trastuzumab (10 μCi in 0.5 ml PBS) was then administered to the mice ($n = 10$–15) 24–30 h later. The tumours were harvested at 6, 24, 48, 72 and 96 h after the last treatment. Mice utilised for the cell cycle and proliferation studies were injected i.p. with 5-bromo-2′-deoxyuridine (BrdU; 1.5 mg in 0.5 ml PBS; Sigma, St Louis, MO, USA) 4 h before euthanasia. The amount of tumour collected was not measured; however, based on previous studies, the tumour burden at 7 d is typically 128.5 ± 205.6 mg (Milenic *et al*, 2010). The tumours at each time point were pooled together, macroscopically inspected, the adherent tissues removed, rinsed in ice-cold PBS, and divided. Tumour tissues were either stored at −80 °C until use or paraffin embedded. Additional groups included tumour-bearing mice that received paclitaxel alone, ^{212}Pb-TCMC-trastuzumab and ^{212}Pb-TCMC-HuIgG with/without paclitaxel pre-treatment, or no treatment. All animal protocols were approved by the National Cancer Institute Animal Care and Use Committee.

Flow cytometry. Cell cycle distribution and DNA synthesis were determined by flow cytometry as previously described with minor modifications (Grégoire *et al*, 1994). Tumour tissues fixed in cold 70% ethanol were prepared and analysed using a FACSCalibur (BD Biosciences, San Jose, CA, USA), collecting 15 000 events excluding cell debris from data collection. The percentage DNA content (propidium iodide) and DNA synthesis (BrdU content) were determined using a two-parameter data collection with CellQuest (BD Biosciences) software, whereas single-parameter DNA distribution was analysed using Modfit LT ver. 3.0 (Verity Software House, Inc, Topsham, ME, USA).

Determination of apoptosis. Apoptotic bodies were scored using hematoxylin and eosin (H&E) staining as described previously using five fields per tumour section, and the number of apoptotic bodies per 100 nuclei scored expressed as a percentage (Stephens *et al*, 1991). Apoptotic bodies were identified using the following criteria: (a) isolated distribution of apoptotic bodies; (b) shrunken cells usually with empty space between neighbouring cells; (c) eosinophilic cytoplasm; (d) condensation of nuclei into dense particles; (e) fragmentation of the nuclei into several bodies; and (f) the absence of inflammatory reaction surrounding the apoptotic cells (non-necrotic cells).

Immunohistochemistry (IHC) and immunofluorscence microscopy. Immunohistochemistry was performed as described in the manufacturer's instructions (Cell Signaling, Danvers, MA, USA) with modifications described elsewhere (Yong *et al*, 2012). Antigen unmasking was performed, at 80 C for 10 min in 10mM sodium citrate. After washing, the washed slides were treated with 3% hydrogen peroxide and incubated for 1 h with 100 μl of Tween-20 in PBS containing 5% normal goat serum. Thereafter, the slides were incubated overnight at 4 °C with either pH3 or γH_2AX antibodies (Cell Signaling) in Tween-20 in PBS with 5% normal goat serum. After washing, the sections were developed with 100 μl 3,3′-diaminobenzidine substrate, dehydrated and coverslips mounted using Cytoseal XYL (Thermo Fisher Scientific, Cincinnati, OH, USA).

Immunofluorescence was performed according to the manufacturer's instructions (Cell signaling). Sections were processed by incubation in blocking solution (1 × PBS/5% normal goat serum/0.3% Triton X-100) for 60 min. The specimens were then incubated overnight at 4 °C with α-tubulin antibody (Cell Signaling, 1 : 100) in PBS/1% BSA/0.3% Triton X-100) After rinsing in PBS three times, the specimens were incubated with a fluorochrome-conjugated secondary (Invitrogen, Carlsbad, CA, USA) antibody for 1 h at room temperature in the dark. After rinsing in PBS, coverslips were mounted using Vectashield (Vector Lab, Burlingame, CA, USA).

Chromatin immunoprecipitation (ChIP). The ChIP assay kit (Upstate Biotechnology, Waltham, MA, USA) was utilised according to the manufacturer's instructions with minor adjustments as previously described (Yong *et al*, 2012). The lysates were prepared and aliquoted. Ten microliter (1 : 100) of each antibody for E2F1 (Upstate Biotechnology) and E2F4 (SantaCruz, Santa Cruz, CA, USA) was added to an aliquot; the resulting DNA–protein complexes were isolated by protein G agarose beads. The samples were subjected to 65 °C for 5 h, the DNA extracted and dissolved in elution reagent. The immunoprecipitated DNA was amplified by PCR using *BubR1* promoter-specific primers (Applied Biosystems, Rockville, MD, USA) and analysed by electrophoresis using 1.5% agarose gels.

Western blotting. Immunoblot analysis following standard procedures was performed with total protein isolates using T-PER tissue protein extraction reagent (Thermo Fisher Scientific) containing protease inhibitors (Roche, Indianapolis, IN, USA). Fifty microgram of total protein per lane was separated on a 4–20% tris-glycine gel and transferred to a nitrocellulose membrane. Antibodies against cleaved pCENP-A (Cell Signaling) and BubR1 (Abcam, Cambridge, MA, USA) were used at a dilution of 1 : 1000 in PBS containing 5% BSA and 0.05% Tween-20. Horseradish peroxidase-conjugated rabbit secondary antibodies were used at 1 : 5000 in 3% non-fat dry milk. The blots were developed using the ECL Plus chemoluminescent detection kit (GE Healthcare, Piscataway, NJ, USA) and the images acquired using a Fuji LAS 4000 imager (Fujifilm, Stamford, CT, USA).

Statistics. A minimum of at least three independent experiments were conducted for each point described. All values were expressed as the mean ± s.d. Student's test was used for paired data, and multiple comparisons were performed with the ANOVA. A P-value <0.05 was considered statistically significant.

RESULTS

α-Radiation from ^{212}Pb may potentiate paclitaxel-induced mitotic catastrophe in human colon carcinoma xenografts. A recent report on the combination of paclitaxel with ^{212}Pb-TCMC-trastuzumab therapy demonstrated the tremendous potential of this combined modality to treat disseminated intraperitoneal disease (Milenic *et al*, 2008). To investigate underlying mechanisms of this potentiation, mice, with a 3-day tumour burden pre-treated with paclitaxel 24 h earlier, were treated with ^{212}Pb-labelled mAb (trastuzumab/HuIgG). The tumours were then collected over a 96-h period as depicted in Figure 1A.

Paclitaxel induces activation of the spindle checkpoint through suppression of microtubule dynamics by binding to the β-subunit of tubulin and stabilising the microtubules. The resultant mitotic arrest triggers rapid onset of the p53-independent apoptotic pathway (Abal *et al*, 2003). Cells treated with paclitaxel undergoing mitotic catastrophe can be identified by the irregular pattern of the mitotic spindle marker, α-tubulin. Consistent with this observation, a moderate degree of microtubule bundling was observed in the tumour tissue from the mice treated with paclitaxel; the data from the 24-h time point is presented as a representative example (Figure 1B and C). In contrast, severe microtubule bundling was observed in the tumour tissues from the mice treated with paclitaxel/^{212}Pb-TCMC-trastuzumab (paclitaxel/^{212}Pb-TCMC-trastuzumab *vs* paclitaxel alone, $P<0.001$). Microtubule bundling is also evident in the tumours from the group of mice treated with

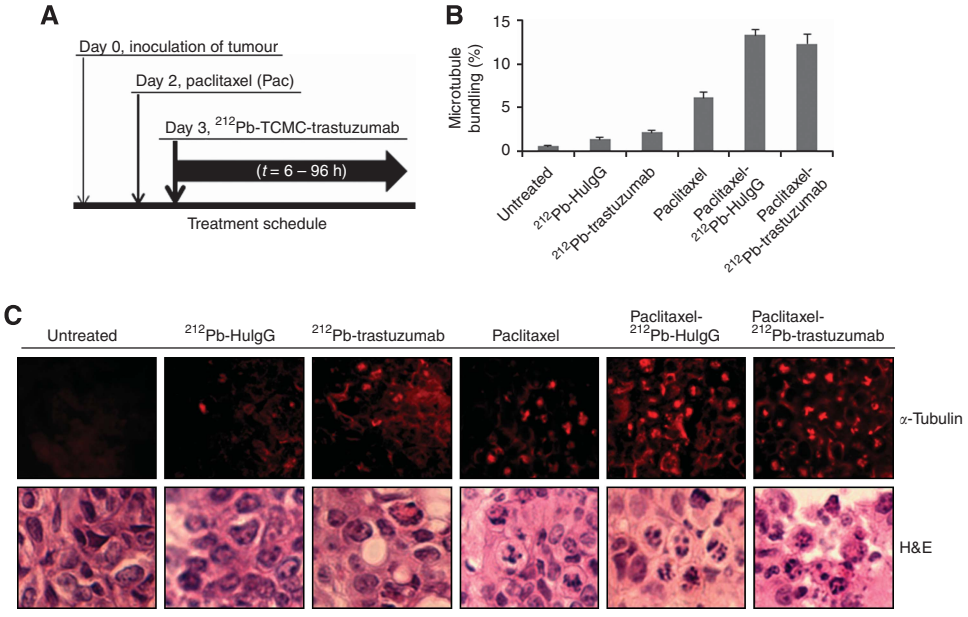

Figure 1. Induction of apoptosis in response to paclitaxel pre-treatment followed by ^{212}Pb-TCMC-trastuzumab in LS-174T i.p. xenografts. (**A**) Schematic of the dual modality treatment schedule. Mice bearing i.p. LS-174T xenografts were treated with paclitaxel followed 24 h later by ^{212}Pb-TCMC-trastuzumab. The tumours were collected over a 96-h period. Additional groups included untreated, paclitaxel alone, ^{212}Pb-TCMC-trastuzumab without paclitaxel pre-treatment and ^{212}Pb-TCMC-HuIgG with/without paclitaxel pre-treatment. (**B**) Microtubule bundling at 24 h induced by ^{212}Pb-TCMC-trastuzumab after paclitaxel treatment 24 h earlier. Paraffin-embedded sections from the indicated time points were stained with α-tubulin and the microtubule bundling was counted under fluorescence microscopy. Results represent the average of a minimum of three replications (± s.d.). (**C**) Fluorescence and light microscopic images of mitotic catastrophe at 24 h. Mice bearing i.p. LS-174T xenografts were treated with paclitaxel followed by ^{212}Pb-TCMC-trastuzumab. Representative paraffin-embedded sections stained for the presence of α-tubulin 24 h after the injection of the ^{212}Pb-labelled trastuzumab and HuIgG are presented (upper panel; α-tubulin staining, ×40). Representative paraffin-embedded sections of the same time point, stained with H&E, are also presented (lower panel; H&E staining). Additional groups included untreated, paclitaxel alone, ^{212}Pb-TCMC-trastuzumab without paclitaxel pre-treatment and ^{212}Pb-TCMC-HuIgG with/without paclitaxel pre-treatment.

paclitaxel/^{212}Pb-TCMC-HuIgG. However, it was not statistically different from paclitaxel/^{212}Pb-TCMC-trastuzumab, suggesting a general effect of α-particle irradiation in response to paclitaxel that cannot be overlooked due to the quantity of ^{212}Pb in the tumour, whether bound to HER2 or not.

Notably, increased multimicronuclei, in other words, mitotic catastrophe, were evident in tumours treated with paclitaxel/^{212}Pb-labelled mAb (trastuzumab/HuIgG) compared with other treatment groups (Figure 1C), supporting the concept that the DNA damage by ^{212}Pb-labelled mAb (trastuzumab/HuIgG) treatment potentiates paclitaxel-induced mitotic catastrophe.

^{212}Pb-TCMC-trastuzumab following pre-treatment with paclitaxel reduces DNA synthesis and induces early G2/M-phase arrest. The effect of paclitaxel/^{212}Pb-TCMC-trastuzumab treatment on DNA synthesis and cell cycle distribution was examined; mice bearing i.p. tumour xenografts were injected with BrdU 4 h before tumour collection. DNA content and BrdU incorporation was then determined by a two-parameter analysis following flow cytometry. A noticeable decrease in BrdU incorporation (8.3 ± 1.2%) was noted at the 6-h time point in tumours from mice treated with paclitaxel/^{212}Pb-TCMC-trastuzumab *vs* the untreated group (23.8 ± 1.3%; Table 1). DNA synthesis decreased further and remained at lower levels thereafter throughout the study period, with no recovery evident. In comparison, DNA synthesis in tumours collected from mice treated with paclitaxel alone was 10.1 ± 1.0% at 6 h; decreasing to 7.8 ± 1.1% at 24 h (paclitaxel/^{212}Pb-TCMC-trastuzumab *vs* paclitaxel alone, $P<0.001$). Depression of DNA synthesis was also observed in the tumours collected from mice that had received paclitaxel/^{212}Pb-TCMC-HuIgG (paclitaxel/^{212}Pb-TCMC-HuIgG *vs* paclitaxel alone, $P<0.001$). However, DNA synthesis appears to be recovering in tumours taken at the 96-h time point from mice that had been injected with either ^{212}Pb-TCMC-HuIgG (^{212}Pb-TCMC-HuIgG at 72 h *vs* ^{212}Pb-TCMC-HuIgG at 96 h, $P<0.05$) or paclitaxel alone (Paclitaxel at 72 h *vs* paclitaxel at 96 h, $P<0.05$).

Next, the effect of the paclitaxel/^{212}Pb-TCMC-trastuzumab treatment regimen on cell cycle was investigated. As expected, cell cycle arrest in the G2/M-phase was evident, at some point, in all tumours except the untreated control and tumours from mice treated with paclitaxel alone (Table 2). Following treatment with paclitaxel/^{212}Pb-TCMC-trastuzumab, an immediate arrest in the G2/M-phase at 6 h was observed that was not displayed by the other treatment groups (paclitaxel/^{212}Pb-TCMC-trastuzumab *vs* paclitaxel alone, $P<0.05$ at 6 h). G2/M-phase arrest in the other treatment groups occurred at 24 h and later. After 24 h, there was a marked decrease in the S-phase compared with the tumour control groups of paclitaxel and untreated mice (paclitaxel/^{212}Pb-TCMC-trastuzumab *vs* paclitaxel alone, $P<0.05$ at 6 h, $P<0.001$ at 24, 48, 72, 96 h; paclitaxel/^{212}Pb-TCMC-HuIgG *vs* paclitaxel alone, $P<0.05$ at 6 h, $P<0.001$ at 48 h and 72 h). By 96 h, the cell cycle distribution in S-phase appears to be rebounding in tumour tissue collected from mice treated with ^{212}Pb-TCMC-HuIgG and paclitaxel/^{212}Pb-TCMC-HuIgG. In contrast, the treatment with ^{212}Pb-TCMC-trastuzumab alone or paclitaxel/^{212}Pb-TCMC-trastuzumab resulted in lower S-phase levels with no recovery evident (Table 2). These results indicate that depression of S-phase and arrest of G2/M-phase seems to be α-radiation specific because tumours collected from mice treated with paclitaxel alone seem to be less affected in cell cycle distribution. However, early G2/M-phase arrest (by 6 h) coupled with sustained S-phase depression appear to be paclitaxel/^{212}Pb-TCMC-trastuzumab treatment specific.

^{212}Pb-TCMC-trastuzumab fails to sustain paclitaxel-induced mitotic arrest and potentiates paclitaxel-induced cell death. Paclitaxel perturbs spindle assembly, which in turn activates the spindle assembly checkpoint, causing mitotic arrest and triggering apoptosis (Jordan and Wilson, 2004). Heavy DNA damage also induces mitotic catastrophe in mammalian cells (Andreassen *et al*, 2001; Chen, 2002). For these reasons, the effect of ^{212}Pb-TCMC-trastuzumab on mitotic spindle checkpoint when the mitotic spindle function was perturbed by paclitaxel was assessed. As an indicator of DNA damage, the paraffin-embedded tumour tissues were stained for γH2AX. A marked increase in positive γH2AX foci staining was observed in tumour tissues treated with ^{212}Pb-TCMC-trastuzumab compared with ^{212}Pb-TCMC-HuIgG following paclitaxel pre-treatment or paclitaxel alone (Figure 2A). At 24 h, paclitaxel induced phospho-histone H3, a major M-phase marker, which accumulates during the M-phase. In contrast, phosphorylation of histone H3 markedly diminished with the combined treatments of paclitaxel and ^{212}Pb-TCMC-trastuzumab, suggesting this treatment regimen might have abrogated the mitotic spindle checkpoint.

Next, apoptosis was assessed by IHC using H&E staining based on the morphological criteria described in the methods. A greater increase in apoptosis was noted at the 6 and 24 h time points for all treatments and time-dependently decreased. At comparable time points, quantitation of the apoptotic bodies indicated that there was an enhanced killing effect in the xenografts from the group of mice pre-treated with paclitaxel and then injected with ^{212}Pb-TCMC-trastuzumab (Figure 2B). This effect achieved significance when compared with paclitaxel/^{212}Pb-TCMC-HuIgG or paclitaxel alone at various time points (paclitaxel/^{212}Pb-TCMC-trastuzumab *vs* paclitaxel alone, $P<0.01$ at 6 and 24 h, $P<0.05$ at 48 and 96 h; paclitaxel/^{212}Pb-TCMC-trastuzumab *vs* paclitaxel/^{212}Pb-TCMC-HuIgG, $P<0.05$ at 6 and 24 h). These results suggest that the DNA damage by ^{212}Pb-RIT (^{212}Pb-trastuzumab) potentiates paclitaxel-induced cell death.

Table 1. Analysis of DNA synthesis in LS-174T tumour xenografts following treatment with paclitaxel and ^{212}Pb-TCMC-trastuzumab

	Time point (h)					
	0	6	24	48	72	96
None	23.8 ± 1.3					
Paclitaxel-^{212}Pb-trastuzumab		8.3 ± 1.2	2.1 ± 1.4	1.7 ± 0.7	1.4 ± 0.5	1.9 ± 0.2
Paclitaxel-^{212}Pb-HuIgG		7.3 ± 1.2	1.3 ± 0.9	1.4 ± 0.1	1.5 ± 0.5	1.8 ± 0.4
Paclitaxel		10.1 ± 1.0	7.8 ± 1.1	6.0 ± 1.3	5.1 ± 1.5	7.6 ± 1.8
^{212}Pb-trastuzumab		13.7 ± 1.2	7.3 ± 1.4	2.6 ± 0.7	7.5 ± 0.5	1.1 ± 0.2
^{212}Pb-HuIgG		16.4 ± 1.2	8.1 ± 0.9	2.4 ± 0.1	2.8 ± 0.5	4.2 ± 0.4

Mice bearing i.p. LS-174T xenografts were treated with ^{212}Pb-TCMC-trastuzumab 24 h after administration of paclitaxel. Four hours before tumour collection, the mice were injected with 5-bromo-2′-deoxyuridine. Additional groups included untreated, paclitaxel alone, ^{212}Pb-TCMC-trastuzumab without paclitaxel pre-treatment and ^{212}Pb-TCMC-HuIgG with/without paclitaxel pre-treatment. Results represent the average of a minimum of three replications (± s.d.).

Table 2. Cell cycle distribution analysis in i.p. tumour xenografts of LS-174T after treatment with paclitaxel and ^{212}Pb-TCMC-trastuzumab RIT

		Time point (h)					
Treatment	**Phase**	**0**	**6**	**24**	**48**	**72**	**96**
	G1	67.5 ± 2.7					
	S	17.7 ± 2.0					
	G2-M	14.8 ± 0.7					
Paclitaxel-^{212}Pb-Trastuzumab	G1		58.9 ± 2.9	67.9 ± 0.2	68.2 ± 1.4	63.9 ± 0.1	75.8 ± 2.7
	S		17.5 ± 3.7	7.6 ± 0.4	6.9 ± 0.1	6.3 ± 0.0	5.5 ± 0.3
	G2-M		23.6 ± 0.8	24.5 ± 0.6	24.9 ± 1.2	29.8 ± 0.0	18.8 ± 3.0
Paclitaxel-^{212}Pb-HulgG	G1		69.3 ± 5.9	56.5 ± 0.4	68.5 ± 0.1	66.3 ± 0.0	64.2 ± 1.7
	S		14.7 ± 0.1	17.8 ± 0.7	5.0 ± 0.2	5.9 ± 0.1	16.1 ± 4.0
	G2-M		16.0 ± 5.8	25.7 ± 0.4	26.5 ± 0.1	27.8 ± 0.1	19.7 ± 2.2
Paclitaxel	G1		63.3 ± 1.5	63.6 ± 0.2	68.1 ± 0.2	68.0 ± 1.6	73.3 ± 0.2
	S		22.1 ± 3.0	18.9 ± 1.0	14.3 ± 0.0	12.4 ± 0.5	11.7 ± 0.5
	G2-M		14.6 ± 1.5	17.5 ± 0.8	17.6 ± 0.2	19.6 ± 1.1	15.1 ± 0.4
^{212}Pb-Trastuzumab	G1		68.6 ± 3.8	66.9 ± 1.3	67.7 ± 4.0	68.1 ± 1.3	66.6 ± 0.7
	S		14.3 ± 5.4	5.9 ± 0.1	6.3 ± 1.8	7.9 ± 0.7	3.6 ± 0.0
	G2-M		17.1 ± 1.6	27.3 ± 1.2	26.1 ± 2.1	23.9 ± 0.6	29.7 ± 0.7
^{212}Pb-HulgG	G1		63.9 ± 5.2	65.1 ± 2.3	64.6 ±	67.1 ± 0.5	63.1 ± 0.3
	S		20.0 ± 5.3	7.4 ± 1.3	5.8 ±	5.5 ± 0.1	7.8 ± 0.7
	G2-M		16.0 ± 0.1	27.5 ± 1.0	29.6 ±	27.4 ± 0.6	29.1 ± 1.0

Abbreviation: RIT = radioimmunotherapy. Mice bearing i.p. LS-174T xenografts were pretreated with paclitaxel before ^{212}Pb-TCMC-trastuzumab RIT. Additional groups included untreated, paclitaxel alone, ^{212}Pb-TCMC-trastuzumab without paclitaxel pretreatment and ^{212}Pb-TCMC-HulgG with/without paclitaxel pre-treatment. Results represent the average of a minimum of three replications (± s.d.).

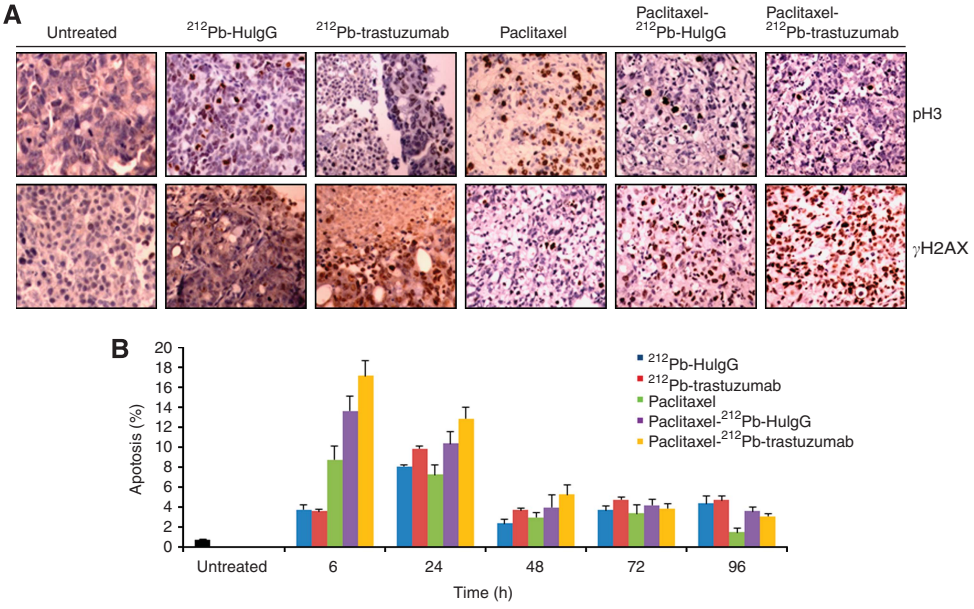

Figure 2. ^{212}Pb-TCMC-trastuzumab-induced inhibition of mitotic checkpoint in LS-174T i.p. xenografts in response to paclitaxel pre-treatment. (**A**) Light microscopic images of paraffin-embedded sections. Mice bearing i.p. LS-174T xenografts were treated with paclitaxel and ^{212}Pb-TCMC-trastuzumab and the tumours harvested from 6 to 96 h post-treatment. Sections were stained with antibodies of pH3 and γH2AX. Additional groups included untreated, paclitaxel alone, ^{212}Pb-TCMC-trastuzumab without paclitaxel pretreatment and ^{212}Pb-TCMC-HulgG with/without paclitaxel pre-treatment. The representative photomicrographs presented are from tumours collected 24 h post treatment, which is 48 h after paclitaxel administration (× 40). (**B**) Apoptosis induced by ^{212}Pb-TCMC-trastuzumab in response to paclitaxel pre-treatment. Paraffin-embedded sections from the indicated time points were stained with H&E and the apoptotic nuclei were counted under light microscopy; 500 nuclei were scored per tumour. Results represent the average of a minimum of three replications (± s.d.).

^{212}Pb-TCMC-trastuzumab treatment may perturb the mitotic spindle checkpoint induced by paclitaxel. The activity of mitotic checkpoint proteins, such as BubR1 and Mad2, has been implicated in the molecular mechanisms of the spindle checkpoint. Phosphorylation of histone H3 facilitates the phosphorylation and recruitment to kinetochores of BubR1 (Bunz *et al*, 1998; Andreassen *et al*, 2001). To better characterise unexplored effects of ^{212}Pb-TCMC-trastuzumab therapy after paclitaxel pre-treatment on mitotic progression, the level of BubR1 protein expression was determined using immunoblot analysis. As shown in Figure 3A, at

24 h, the BubR1 expression was markedly reduced upon treatment with paclitaxel/^{212}Pb-TCMC-trastuzumab (paclitaxel/^{212}Pb-TCMC-trastuzumab *vs* paclitaxel alone, $P<0.001$; paclitaxel/^{212}Pb-TCMC-HuIgG *vs* paclitaxel, $P<0.001$), suggesting that the mitotic spindle checkpoint induced by paclitaxel may be impaired by ^{212}Pb-TCMC-trastuzumab treatment. The affinity of BubR1, not Mad2, for kinetochores is directly influenced by the absence or presence of the survivin/Aurora B complex chromosomal passenger proteins. For this reason, the effect of paclitaxel/^{212}Pb-TCMC-trastuzumab on maintenance of a stable genome was examined. The phosphorylation status of CENP-A (pS7), a surrogate marker of Aurora kinase activity, was determined using western blot analysis. Phosphorylation of CENP-A (pS7), indicative of activated Aurora B, in tumour tissues from mice treated with paclitaxel and ^{212}Pb-TCMC-trastuzumab was diminished (Figure 3A). In contrast, no significant changes in the phosphorylation of CENP-A were observed in tumour tissues from mice treated with paclitaxel, suggesting that ^{212}Pb-TCMC-trastuzumab may interfere with the affinity of BubR1 for kinetocores, thus perturbing the mitotic spindle checkpoint induced by paclitaxel.

E2F is involved in DNA replication, DNA repair and mitosis, suggesting E2F affects cell cycle progression both at S-phase and during mitosis. BubR1 has transcription-binding sites for E2F transcription factors (Chen, 2002). To investigate whether these transcription factors may mediate a decrease of BubR1 expression by recruitment of transcription factor, E2Fs to the *BubR1* proximal promoter region, the binding of E2F1 and E2F4 to the proximal *BubR1* promoter was evaluated using a ChIP assay. Results showed that no significant binding with E2F1 was elicited by any of the treatments. In contrast, enhanced E2F4 binding to the *BubR1* promoter was observed in mice treated with the paclitaxel/^{212}Pb-TCMC-trastuzumab (Figure 3B), suggesting that ^{212}Pb-TCMC-trastuzumab may repress the expression of mitotic checkpoint gene, *BubR1*. Modulation of this gene may be occurring via the increased binding of the repressive transcription factor, E2F4, to the proximal promoter region.

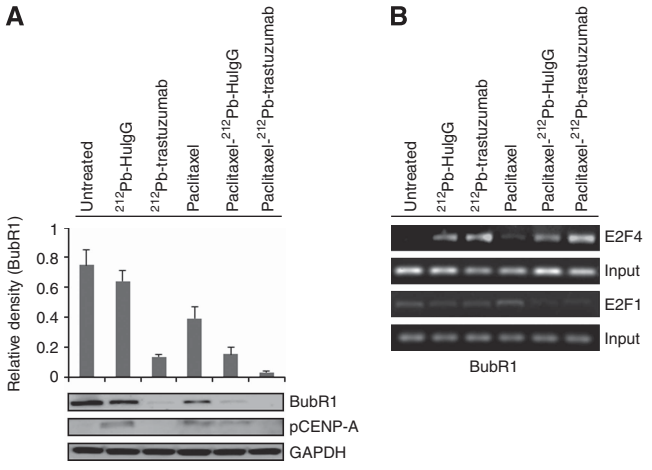

Figure 3. ^{212}Pb-TCMC-trastuzumab effect with paclitaxel pre-treatment on mitotic spindle checkpoint in LS-174T i.p. xenografts. (**A**) Downregulation of BubR1 by ^{212}Pb-TCMC-trastuzumab in response to paclitaxel. Mice bearing i.p. LS-174T xenografts were treated with ^{212}Pb-TCMC-trastuzumab following treatment with paclitaxel 24 h earlier. Additional groups included untreated, paclitaxel alone, ^{212}Pb-TCMC-trastuzumab without paclitaxel pretreatment and ^{212}Pb-TCMC-HuIgG with/without paclitaxel pretreatment. Western blot analysis for BubR1 and pCENP-A was performed with tumour samples collected 24 h after treatment (48 and 24 h post-injection of paclitaxel and ^{212}Pb-TCMC-trastuzumab, respectively). The BubR1 was detected at 130 kDa and the pCENP-A was detected at 17 kDa. Equal protein loading control was GAPDH. (**B**) Downregulation of BubR1 mediated by transcription factor, E2F4. Mice bearing i.p. LS-174T xenografts were treated with paclitaxel followed 24 h later by ^{212}Pb-TCMC-trastuzumab. ChIP assay was performed and PCR-amplified using *BubR1* promoter-specific primer. Electrophoresis was performed using 1.5% agarose gels.

DISCUSSION

Paclitaxel is an attractive candidate chemotherapeutic agent for combination with radiation therapy. *In vivo,* paclitaxel has been shown to enhance the radiation response of murine mammary carcinoma when given up to 24 h before low-LET radiotherapy (Milas *et al*, 1994). The combination of paclitaxel and radiotherapy was shown to increase mitotically arrested tumour cells with a corresponding increase in apoptosis. This laboratory has recently reported on the potentiation of the HER2-binding high-LET radiation agent ^{212}Pb-TCMC-trastuzumab by paclitaxel (Milenic *et al*, 2008). The therapeutic efficacy of ^{212}Pb-TCMC-trastuzumab treatment was impressive when paclitaxel was given 24 h before ^{212}Pb-TCMC-trastuzumab. In this study, the molecular mechanisms associated with the sensitisation or potentiation effect of paclitaxel on ^{212}Pb-TCMC-trastuzumab therapy were investigated.

Anti-mitotic drugs work by perturbing spindle assembly, activating the spindle assembly checkpoint, causing mitotic arrest and triggering apoptosis. Therapy with ^{212}Pb-TCMC-trastuzumab following paclitaxel pre-treatment resulted in an increase in the number of cells with atypically distributed tubulin subunits. Such a phenomenon has been described in cells undergoing mitotic catastrophe, which is a term used to describe the failure of mitosis caused by chromosome missegregation (Roninson *et al*, 2001). The induction of mitotic catastrophe with abnormal mitotic cells may result in cell death. The combination of ^{212}Pb-TCMC-trastuzumab with paclitaxel also elicited an additive effect on mitotic catastrophe and apoptosis. Thus, paclitaxel/^{212}Pb-TCMC-trastuzumab treatment induced both increased mitotic catastrophe and apoptosis in the colon cancer xenograft model utilised in these studies.

The sensitising effect of ^{212}Pb-TCMC-trastuzumab treatment on paclitaxel-induced cell death appears to be accompanied by alterations in the cell cycle. Combination of ^{212}Pb-TCMC-trastuzumab with paclitaxel pre-treatment resulted in an early arrest in the G2/M phase, which remained throughout the 96-h study period. Concurrently, diminished levels of DNA synthesis and depressed S-phase were observed following the treatment regimen of paclitaxel/^{212}Pb-TCMC-trastuzumab, occurring at early time points and persisting throughout the 96-h study period. Although similar G2/M-phase arrest and depressed S-phase were observed for the tumours in mice treated with both ^{212}Pb-mAb (trastuzumab/HuIgG) and paclitaxel/ ^{212}Pb-mAb (trastuzumab/HuIgG), tumours from mice given ^{212}Pb-TCMC-HuIgG or paclitaxel/^{212}Pb-TCMC-HuIgG were beginning to exhibit recovery of the S-phase at 96 h. Similar effects have been observed in our earlier studies (Yong *et al*, 2012, 2013). Interestingly, rebound of the cell cycle in the group that received paclitaxel and ^{212}Pb-HuIgG appears greater than that of the group that received ^{212}Pb-HuIgG alone. It is unclear why the rebound appears to occur and studies are needed to investigate this specific observation. No recovery was evident in the tumours collected from the mice given ^{212}Pb-TCMC-trastuzumab or paclitaxel/^{212}Pb-TCMC-trastuzumab. Synchronisation in the G2/M-phase after 96 h, together with persistent reduced DNA synthesis and depressed S-phase, appears as the most prominent difference between targeted ^{212}Pb-TCMC-trastuzumab and the nonspecific control, ^{212}Pb-TCMC-HuIgG. This suggests that the observed effects are specific to ^{212}Pb-TCMC-trastuzumab. The powerful arrest of cells in the G2/M phase is

thought to account for the reported synergy between paclitaxel and radiation (Asosingh *et al*, 2003). There appears to be an increase in the percent DNA synthesis for ^{212}Pb-TCMC-trastuzumab at 72 h. The increase is transient and unexpected. Additional studies will be performed to further investigate this observation.

High LET radiation from an α-emitting radionuclide is thought to result in irreparable double-stranded DNA breaks and severe chromosomal damage leading to the rapid induction of apoptosis and cell death (Yong and Brechbiel, 2011). Enhancement of α-particle RIT cytotoxicity by paclitaxel through cell cycle arrest and increased DNA double breaks has been observed *in vitro* (Supiot *et al*, 2005). DNA damage induces mitotic catastrophe in mammalian cells that results in the formation of cells with two or more nuclei. A robust mitotic spindle checkpoint potentially allows for repair of chromosomal damage and to effect their proper alignment; whereas inactivation of the spindle checkpoint leads to rapid cell death. Compared with paclitaxel alone, paclitaxel/^{212}Pb-TCMC-trastuzumab treatment increased the phosphorylation of γH2AX indicating increased DNA damage, as well as diminished phosphorylation of histone H3, suggesting that the mitotic spindle checkpoints might have been perturbed.

Proper chromosome segregation relies on the action of the spindle checkpoint. Phosphorylation of histone H3 appears to be coincident with and possibly facilitates phosphorylation and recruitment to kinetochores of the mitotic checkpoint protein, BubR1 (Ota *et al*, 2002; Ditchfield *et al*, 2003; Hauf *et al*, 2003). The survivin/Aurora B complex directly influences BubR1 affinity and is essential for chromosome biorientation, a prerequisite for proper chromosome segregation. Notably, paclitaxel/^{212}Pb-TCMC-trastuzumab treatment interferes with Aurora B kinase, as evidenced by reduction of pCENP-A (pS7), a marker of Aurora kinase activity, and correlates with the diminished phosphorylation of histone H3. Paclitaxel/^{212}Pb-TCMC-trastuzumab treatment had the greatest effect on the mitotic spindle checkpoint proteins investigated. Therefore, the data presented herein indicate that tumours pre-sensitised with paclitaxel before the administration of ^{212}Pb-TCMC-trastuzumab RIT had the greatest effect on the displacement of mitotic spindle checkpoint proteins from the kinetochore. This displacement may be due to inactivation of kinases requisite in mitosis, such as the Aurora B kinase, or lack of a functional survivin/Aurora B complex. Lack of BubR1 localisation to kinetochores has been associated with the mitotic spindle checkpoint inactivation and increased cell death (Dai *et al*, 2004; Lee *et al*, 2004). BubR1 is also involved in regulation of DNA damage responses and has an important role in mediating the cross-talk between the spindle checkpoint and the DNA damage checkpoint (Fang *et al*, 2006). The studies described here addressed the question as to whether or not the decrease in the BubR1 protein was accompanied by an increase in binding of transcriptional repressor protein. The downregulation of *BubR1,* the E2F target gene, was a result of active repression by recruitment of E2F4 to the gene promoters, suggesting that ^{212}Pb-TCMC-trastuzumab combined with paclitaxel may enhance cytotoxicity through perturbation of the mitotic spindle checkpoint protein, BubR1, which may be mediated by association with a transcription factor, E2F4.

Irradiated cells release signals and induce responses in cells whose nuclei were not hit by radiation, resulting in genetic damage, genomic instability or cell death. A high apoptotic rate was also observed for the nonspecific control Paclitaxel-^{212}Pb-TCMC-HuIgG-treated group. For α-particle irradiation, the micronucleus induction has a biphasic phenomenon containing a low-dose hypersensitivity characteristic and its dose response could be well simulated with a state vector model where radiation-induced bystander effects are involved. The increase in the micronucleus frequency in bystander cells (an indication of DNA misrepair or chromosomal breakage) provides evidence for the indirect DNA damage signal or a bystander phenomenon released by irradiated cells. The bystander effect may be a potentially harmful or a useful event in radiotherapy. The nonspecific effect in α-particle RIT may occur just as it does with β^--emitter therapy. Therefore, consideration must be given to these bystander effects of radiation because transmissible biological effects resulting from the radiation insult are pronounced following high LET radiation, such as α-particle irradiation.

The prior therapy study showed that the nonspecific treatment, paclitaxel/^{212}Pb-TCMC-HuIgG, does have an effect on median survival (ms). 2.8-x the untreated control and 2-x the ms of ^{212}Pb-TCMC-HuIgG alone (Milenic *et al*, 2008). Without paclitaxel, only a 1.4-fold enhancement is achieved with ^{212}Pb-TCMC-HuIgG. The ms of paclitaxel/^{212}Pb-TCMC-trastuzumab was 10.7-x that of the untreated control. Thus, the combination of α-irradiation and paclitaxel does enhance therapy albeit at a lower level for the nonspecific material. The level of therapy enhancement achieved by paclitaxel/^{212}Pb-trastuzumab is significantly higher. Some of the differences at the molecular level described may be small, but significant compared with the therapy enhancement. It must be mentioned that the radioactivity is administered i.p., thus significant α-irradiation of tumour tissue does occur even with the nonspecific ^{212}Pb-TCMC-HuIgG. It is possible that, the *in vivo* environment being complex, the magnitude of the molecular test results is approaching limiting levels of detectability making differences harder to discern. Nonetheless, there is no doubt that the combination of α-irradiation and paclitaxel results in discernible differences at the molecular level compared with the controls and may in part explain the therapy experience.

In summary, ^{212}Pb-TCMC-trastuzumab treatment in response to paclitaxel may interfere with a functional Aurora B, which reduces the affinity of BubR1 for kinetochores, leading to the impairment of the mitotic spindle checkpoint and committing tumour cells to death. Pre-clinical *in vitro* (cell culture) or *in vivo* (animal tumour models) studies still remain limited in their ability to permit predictions of actual therapeutic responses in humans. However, the findings reported here provide a mechanistic understanding of how α-emitter RIT combined with paclitaxel enhances the efficacy of specific treatments in the xenograft model presented. A solid rational for combining targeted α-emitter RIT with paclitaxel that includes efficacy and understanding of mechanism may promote clinical translation and provide new prospects for the treatment and management of cancer patients with disseminated peritoneal disease.

ACKNOWLEDGEMENTS

This research was supported in part by the Intramural Research Program of the NIH, National Cancer Institute, Center for Cancer Research and also by AREVA Med.

CONFLICT OF INTEREST

The authors declare no conflict of interest

REFERENCES

Abal M, Andreu JM, Barasoain I (2003) Taxanes: microtubule and centrosome targets, and cell cycle dependent mechanisms of action. *Curr Cancer Drug Targets* **3**: 193–203.

Agus DB, Bunn Jr PA, Franklin W, Garcia M, Ozols RF (2000) HER2/neu as a therapeutic target in non-small cell lung cancer, prostate cancer, and ovarian cancer. *Semin Oncol* **27**: 53–63.

Andreassen PR, Lacroix FB, Lohez OD, Margolis RL (2001) Neither p21WAF1 nor 14-3-3sigma prevents G2 progression to mitotic catastrophe in human colon carcinoma cells after DNA damage, but p21WAF1 induces stable G1 arrest in resting tetraploid cells. *Cancer Res* **61**: 7660–7668.

Asosingh K, De Raeve H, Van Riet I, Van Camp B, Vanderkerken K (2003) Multiple myeloma tumor progression in the 5T2MM murine model is a multistage and dynamic process of differentiation, proliferation, invasion, and apoptosis. *Blood* **101**: 3136–3141.

Bunz F, Dutriaux A, Lengauer C, Walsman T, Zhou S, Brown JP, Sedivy JM, Kinzler KW, Vogelstein B (1998) Requirement for p53 and p21 to sustain G2 arrest after DNA damage. *Science* **282**: 1497–1501.

Burke PA, DeNardo SJ, Miers LA, Kukis DL, DeNardo GL (2002) Combined modality radioimmunotherapy. Promise and peril. *Cancer* **94**: 1320–1331.

Chappell LL, Dadachova E, Milenic DE, Gamestani K, Wu C, Brechbiel MW (2000) Synthesis, characterization, and evaluation of a novel bifunctional chelating agent for the lead isotopes [203]Pb and [212]Pb. *Nucl Med Biol* **27**: 93–100.

Chen RH (2002) BubR1 is essential for kinetochore localization of other spindle checkpoint proteins and its phosphorylation requires Mad1 *J Cell Biol* **158**: 487–496.

Chung HW, Bang SM, Park SW, Chung JB, Kang JK, Kim JW, Seong JS, Lee WJ, Song SY (2004) A prospective randomized study of gemcitabine with doxifluridine versus paclitaxel with doxifuridine in concurrent chemoradiotherapy for locally advanced pancreatic cancer. *Int J Radiat Oncol Biol Phys* **60**: 1494–1501.

Clarke K, Lee FT, Brechbiel MW, Smyth FE, Old LJ, Scott AM (2000) Therapeutic efficacy of anti-Lewis(y) humanized 3S193 radioimmunotherapy in a breast cancer model: enhanced activity when combined with taxol chemotherapy. *Clin Cancer Res* **6**: 3621–3628.

Crow DM, Williams L., Colcher D, Wong JY, Raubitschek A, Shively JE (2005) Combined radiotherapy and chemotherapy of breast tumors with Y-90-labeled anti-Her2 and anti-CEA antibodies with Taxol. *Bioconjug Chem* **16**: 1117–1125.

Dadachova E, Chappell LL, Brechbiel MW (1999) Spectrophotometric method for determination of bifunctional macrocyclic ligands in macrocyclic ligand-protein conjugates. *Nucl Med Biol* **26**: 977–982.

Dai W, Wang Q, Lin T, Swamy M, Fang Y, Xie S, Mahmood R, Yang YM, Rao CV (2004) Slippage of mitotic arrest and enhanced tumor development in mice with BubR1 haploinsufficiency. *Cancer Res* **64**: 440–445.

Dickler A, Abrams RA (2005) Radiochemotherapy in the management of pancreatic cancer-Part II: use in adjuvant and locally unresectable settings. *Semin Radiat Oncol* **15**: 235–244.

Ditchfield C, Johnson VL, Tighe A, Ellston R, Haworth C, Johnson T, Mortlock A, Keen N, Taylor SS (2003) Aurora B couples chromosome alignment with anaphase by targeting BubR1, Mad2, and Cenp-E to kinetochores. *J Cell Biol* **161**: 267–280.

Fang Y, Liu T, Wang YM, Yang YM, Deng H, Kunicki J, Traganos F, Darzynkiewicz Z, Lu L, Dai W (2006) BurbR1 is involved in regulation of DNA damage responses. *Oncogene* **25**: 3598–3605.

Friesen C, Glatting G, Koop B, Schwarz K, Morgenstern A, Apostolidis C, Debatin KM, Reske SN (2007) Breaking chemoresistance and radioresistance with [213]Bi anti-CD45 antibodies in leukemia cells. *Cancer Res* **67**: 1950–1958.

Grégoire V, Van NT, Stephens LC, Brock WA, Milas L, Plunkett W, Hittelman WN (1994) The role of fludarabine-induced apoptosis and cell cycle synchronization in enhanced murine tumor radiation response *in vivo*. *Cancer Res* **54**: 6201–6209.

Hauf S, Cole RW, LaTerra S, Zimmer C, Schnapp G, Walter R, Heckel A, van Meel J, Rieder CL, Peters JM (2003) The small molecule Hesperadin reveals a role for Aurora B in correcting kinetochore-microtubule attachment and in maintaining the spindle assembly checkpoint. *J Cell Biol* **161**: 281–294.

Jemal A, Siegel R, Ward E, Murray T, Xu J, Thun MJ (2007) Cancer Statistics, 2007. *CA Cancer J Clin* **57**: 43–66.

Jordan MA, Wilson L (2004) Microtubules as a target for anticancer drugs. *Nat Rev Cancer* **4**: 253–265.

Kelly MP, Lee FT, Tahtis K, Smyth FE, Brechbiel MW, Scott AM (2007) Radioimmunotherapy with α-particle emitting [213]Bi-C-funtionized trans-cyclohexyl-diethylentriaminepentacetic acid-humanized 3S193 is enhanced by combination with paclitaxel chemotherapy. *Clin Cancer Res* **13**: 5604s–5612s.

Ko AH, Tempero MA (2005) Systemic therapy for pancreatic cancer. *Semin Radiat Oncol* **15**: 245–253.

Lee EA, Keutmann MK, Dowling KL, Harris E, Chan G, Kao GD (2004) Inactivation of mitotic checkpoint as a determinant of the efficacy of microtubule-targeted drugs in killing human cancer cells. *Mol Cancer Ther* **3**: 661–669.

Lee S, Yang W, Lan KH, Sellappan S, Klos K, Hortobagyi G, Hung MC, Yu D (2002) Enhanced sensitization to taxol-induced apoptosis by herceptin pretreatment in ErbB2-overexpressing breast cancer cells. *Cancer Res* **62**: 5703–5710.

Liebmann J, Cook JA, Fisher J, Teague D, Mitchell JB (1994) *In vitro* studies of Taxol as a radiation sensitizer in human tumor cells. *J Natl Cancer Inst* **86**: 441–446.

Lowry OH, Rosebrough NJ, Farr AL, Randall RJ (1951) Protein measurement with the Folin phenol reagent. *J Biol Chem* **193**: 265–275.

Meredith RF, Buchsbaum DJ, Alvarez RD, LoBuglio AF (2007) Brief overview of preclinical and clinical studies in the development of intraperitoneal radioimmunotherapy for ovarian cancer. *Clin Cancer Res* **13**: 5643s–5645s.

Milas L, Hunter NR, Mason KA, Kurdoglu B, Peter LJ (1994) Enhancement of tumor radioresponse of murine mammary carcinoma by paclitaxel. *Cancer Res* **54**: 3506–3510.

Milenic DE, Garmestani K, Brady ED, Albert PS, Abdulla A, Flynn J, Brechbiel MW (2007) Potentiation of high-LET radiation by gemcitabine: targeting HER2 with trastuzumab to treat disseminated peritoneal disease *Clin Cancer Res* **13**: 1926–1935.

Milenic DE, Garmestani K, Brady ED, Baidoo KE, Albert PS, Wong KJ, Brechbiel MW (2008) Multimodality therapy: potentiation of high linear energy transfer radiation with paclitaxel for the treatment of disseminated peritoneal disease. *Clin Cancer Res* **14**: 5108–5115.

Milenic DE, Garmestani K, Bardy ED, Albert PS, Ma D, Abdulla A, Brechbiel MW (2004) Targeting of HER2 antigen for the treatment of disseminated peritoneal disease. *Clin Cancer Res* **10**: 7834–7841.

Milenic DE, Garmestani K, Brady ED, Albert PS, Ma D, Abdulla A, Brechbiel MW (2005) Alpha-particle radioimmunotherapy of disseminated peritoneal disease using a [212]Pb-labeled radioimmunoconjugate targeting HER2. *Cancer Biother Radiopharm* **20**: 557–568.

Milenic DE, Wong KJ, Baidoo KE, Nayak TK, Regino CA, Gamestani K, Brechbiel MW (2010) Targeting HER2: a report on the *in vitro* and *in vivo* preclinical data supporting trastuzumab as a radioimmunoconjugate for clinical trials. *Mabs* **2**: 550–564.

Ota T, Suto S, Katayama H, Han ZB, Suzuki F, Maeda M, Tanino M, Terada Y, Tatsuka M (2002) Increased mitotic phosphorylation of histone H3 attributable to AIM-1/Aurora B overexpression contributes to chromosome number instability. *Cancer Res* **62**: 5168–5177.

Rodriguez M, Sevin BU, Perras J, Nauyen HN, Pham C, Stern AJ, Koechli OR, Averette HE (1995) Paclitaxel: a radiation sensitizer of human cervical cancer cells. *Gynecol Oncol* **57**: 165–169.

Roninson IB, Broude EV, Chang BD (2001) If not apoptosis, then what? Treatment-induced mitotic catastrophe in tumor cells. *Drug Resist Updat* **4**: 303–313.

Stephens LC, Ang KK, Schultheiss TE, Milas L, Meyn RE (1991) Apoptosis in irradiated murine tumors. *Radiat Res* **127**: 308–316.

Steren A, Sevin BU, Perras J, Ramos R, Angioli R, Nguyen H, Koechli O, Averette HE (1993) Taxol as a radiation sensitizer: a flow cytometric study. *Gynecol Oncol* **50**: 89–93.

Supiot S, Gouard S, Charrier J, Apostolidis C, Chatal JF, Barbet J, Davodeau F, Cherel M (2005) Mechanisms of cell sensitization to alpha radioimmunotherapy by doxorubicin or paclitaxel in multiple myeloma cell lines. *Clin Cancer Res* **11**: 7047s–7052s.

Tom BH, Rutzky LP, Jakstys MM, Oyasu R, Kaye CI, Kahan BD (1976) Human colonic adenocarcinoma cells. I. Establishment and description of a new cell line. *In Vitro* **12**: 180–191.

Yong K, Brechbiel MW (2011) Towards translation of [212]Pb as a clinical therapeutic; getting the lead in! *Dalton Trans* **40**: 6068–6076.

Yong KJ, Milenic DE, Baidoo KE, Brechbiel MW (2012) [212]Pb-Radioimmunotherapy induces G2 cell cycle arrest and delays DNA damage repair in tumor xenografts in a model for disseminated intraperitoneal disease. *Mol Cancer Ther* **11**: 639–648.

Yong KJ, Milenic DE, Baidoo KE, Brechbiel MW (2013) Sensitization of tumor to [212]Pb-radioimmunotherapy by gemcitabine involves initial abrogation of G2 arrest and blocked DNA damage repair by interference with Rad51. *Int J Radiat Oncol Biol Phys* **85**: 1119–1126.